



Supplementary Information for

Fluctuating auxin response gradients determine pavement cell shape acquisition

Peter GRONES, Mateusz MAJDA, Siamsa M. DOYLE, Daniël VAN DAMME, Stéphanie ROBERT

Stéphanie ROBERT

Email: Stephanie.Robert@slu.se

This PDF file includes:

Figures S1 to S8

Tables S1

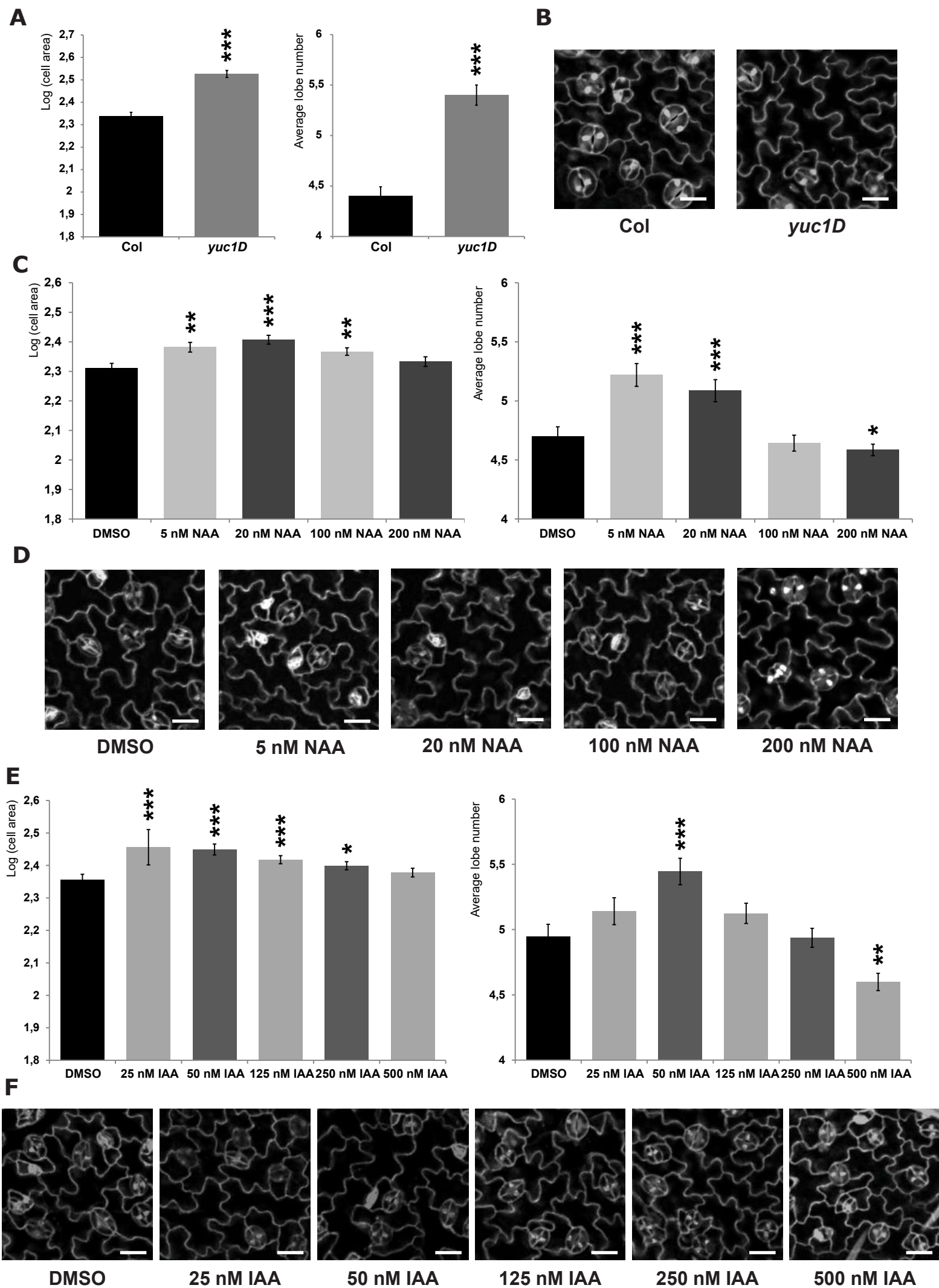


Figure S1.

Fig. S1. Auxin regulates pavement cell lobe formation in a dose-dependent manner. (A) Graphs representing the log cell area and average lobe number of analysed cells of the 3rd leaf in two-week-old *Arabidopsis* in wild type (Col) and *yuc1D* auxin overproducing mutant. n = 621 (Col) and 721 (*yuc1D*) cells. (B) Representative images of leaf epidermal cells of wild type (Col) and *yuc1D* auxin overproducing mutant. (C) Quantification of the log cell area and average lobe number in wild type pavement cells after mock (DMSO) and 5 nM, 20 nM, 100 nM and 200 nM NAA treatment. n = 1039 (DMSO), 956 (5 nM), 943 (20 nM), 1146 (100 nM) and 603 (200 nM) cells. (D) Representative images of wild type leaf epidermal cells after mock treatment (DMSO) and different NAA treatments. (E) Quantification of the log cell area and average lobe number in pavement cells after mock (DMSO) and 25 nM, 50 nM, 125 nM, 250 nM and 500 nM IAA treatment. n = 918 (DMSO), 847 (25 nM), 798 (50 nM), 1212 (125 nM), 1142 (250 nM), 1204 (500 nM). (F) Representative images of wild type leaf epidermal cells after mock treatment (DMSO) and different IAA treatments. Error bars correspond to \pm s.e. Statistical significance compared to DMSO mock-treated cells or Col tested by Wilcoxon test (*P < 0.05; **P < 0.01; ***P < 0.001). Scale bar = 20 μ m.

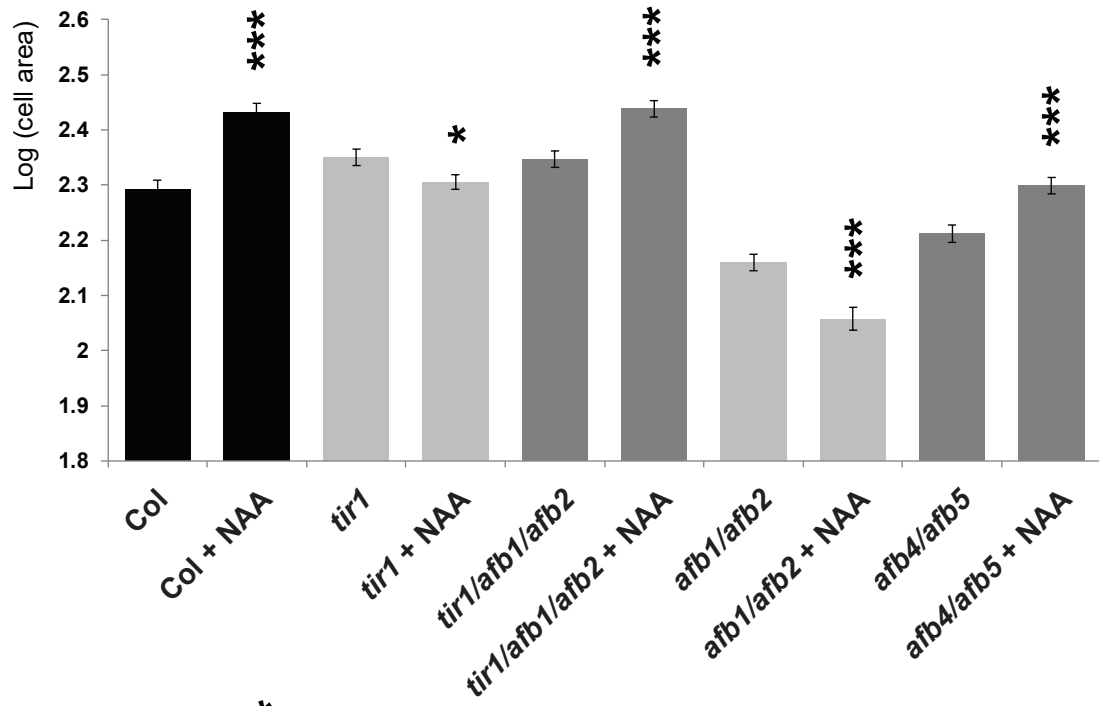
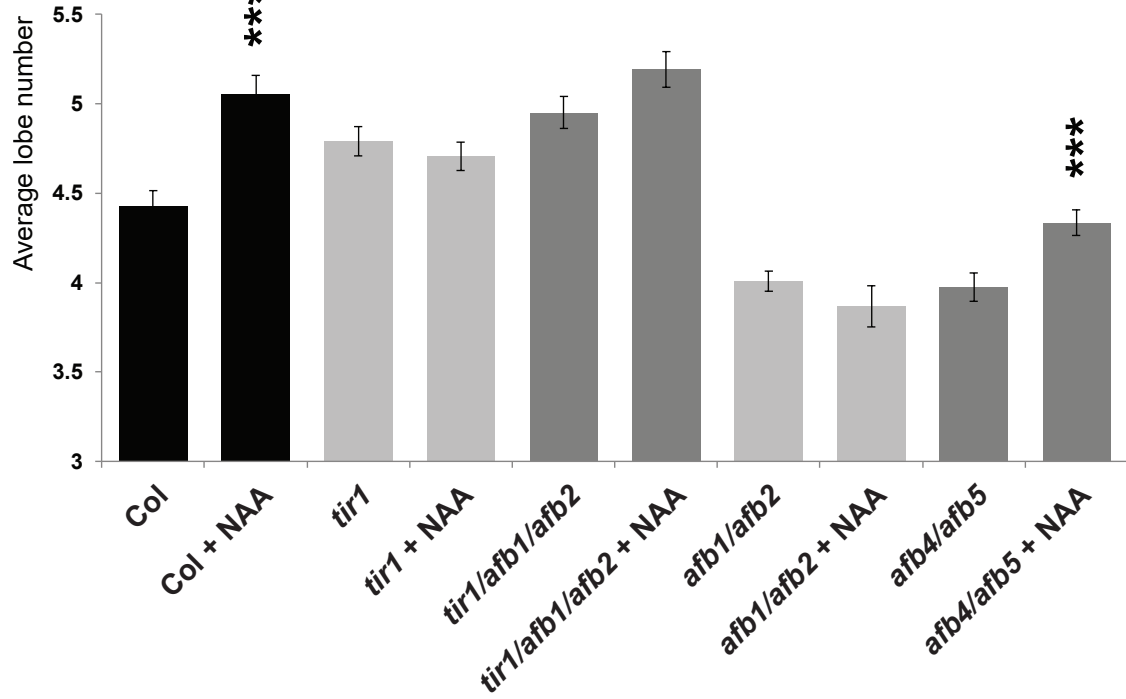
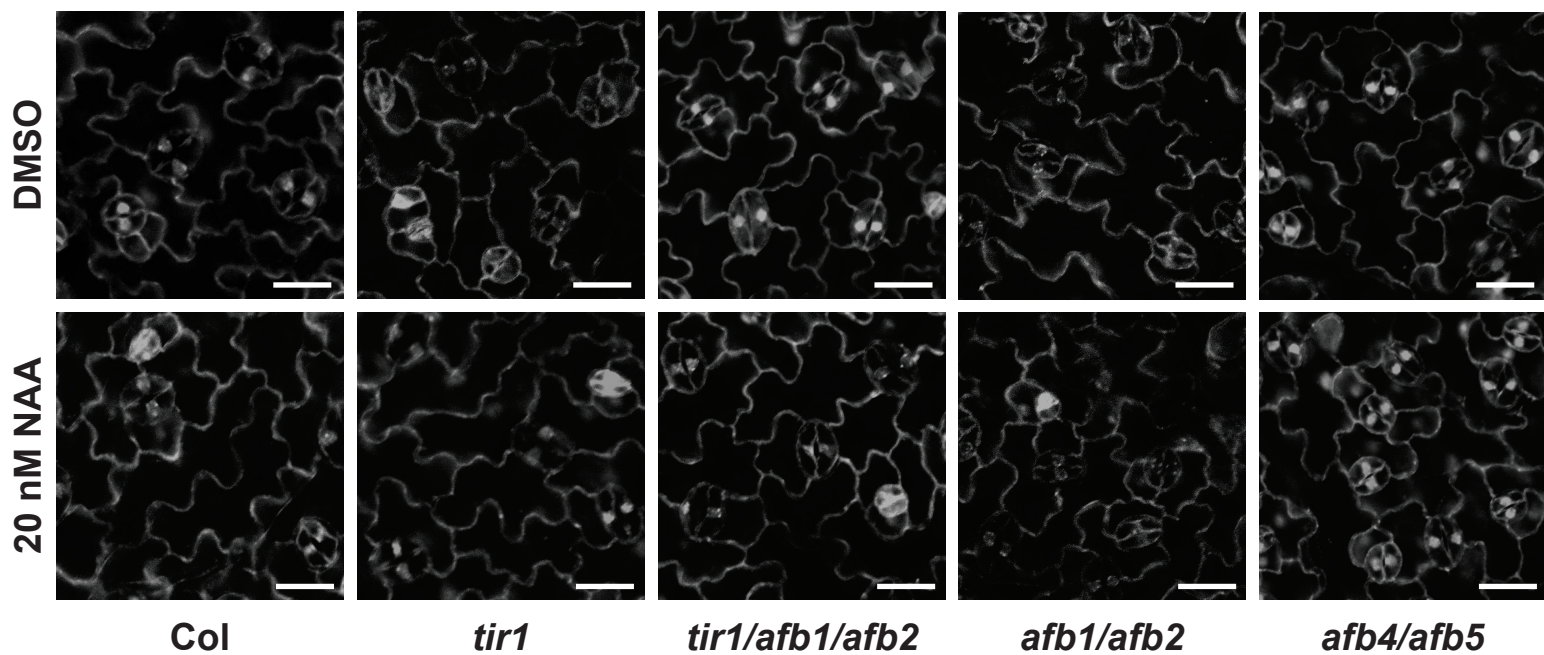
A**B****C**

Fig. S2. Nuclear auxin signaling is involved in auxin-mediated pavement cell lobe formation. (A-B) Graphs representing the log cell area and average lobe number of analyzed cells of the 3rd leaf in two-week-old *Arabidopsis* in wild type (Col) and different *tir/afb* mutants after mock (DMSO) or 20 nM NAA treatment. n = 571 (Col), 611 (Col+NAA), 907 (*tir1*), 948 (*tir1*+NAA), 875 (*tir1/afb1/afb2*), 725 (*tir1/afb1/afb2*+NAA), 653 (*afb1/afb2*), 717 (*afb1/afb2*+NAA), 955 (*afb4/afb5*) and 750 (*afb4/afb5*+NAA). (C) Representative images of leaf epidermal cells in different *tir/afb* mutants after mock (DMSO) and 20 nM NAA treatments. Error bars correspond to \pm s.e. Statistical significance compared to DMSO mock-treated cells or Col tested by Wilcoxon test (*P < 0.05; ***P < 0.001). Scale bar = 20 μ m.

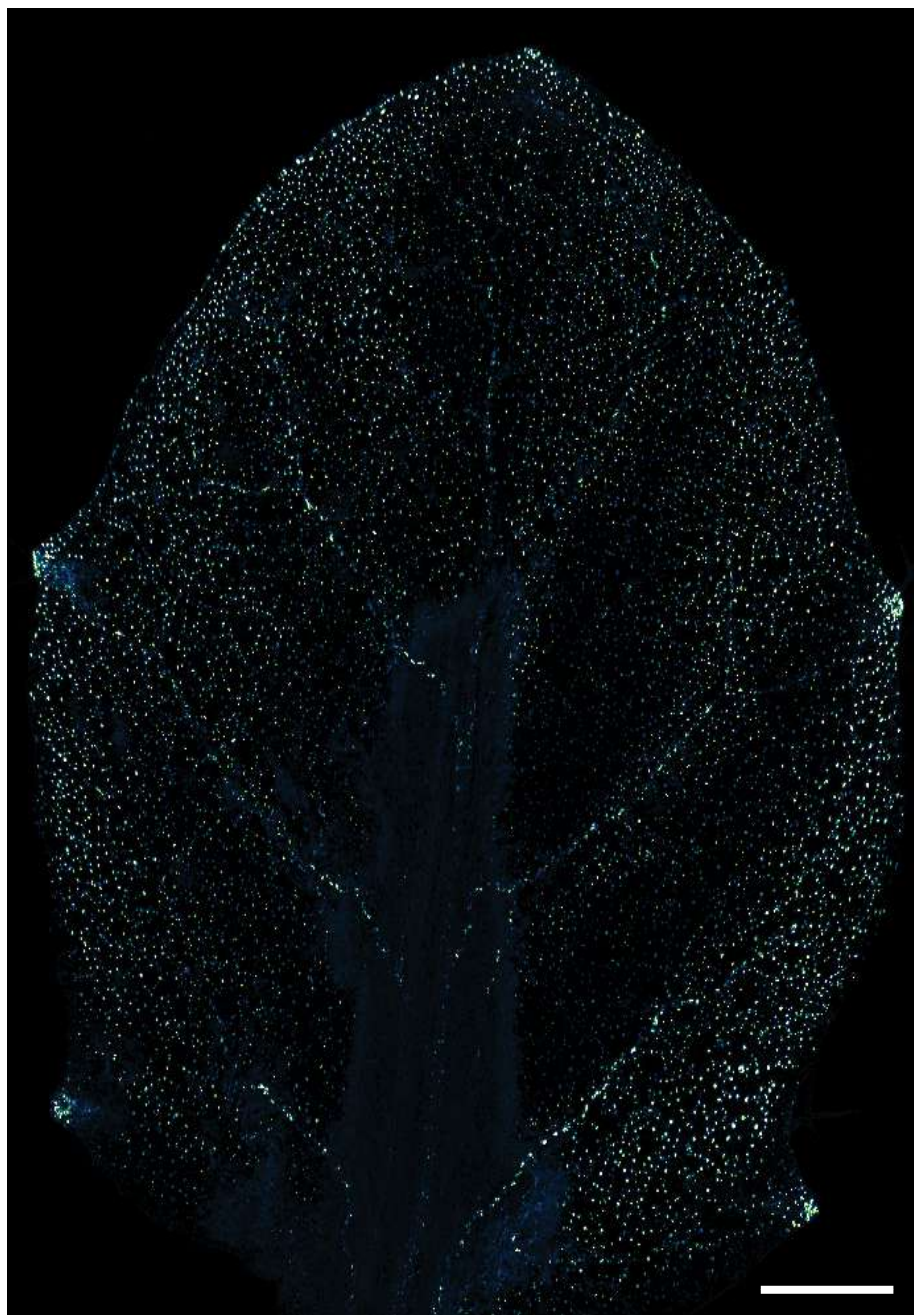
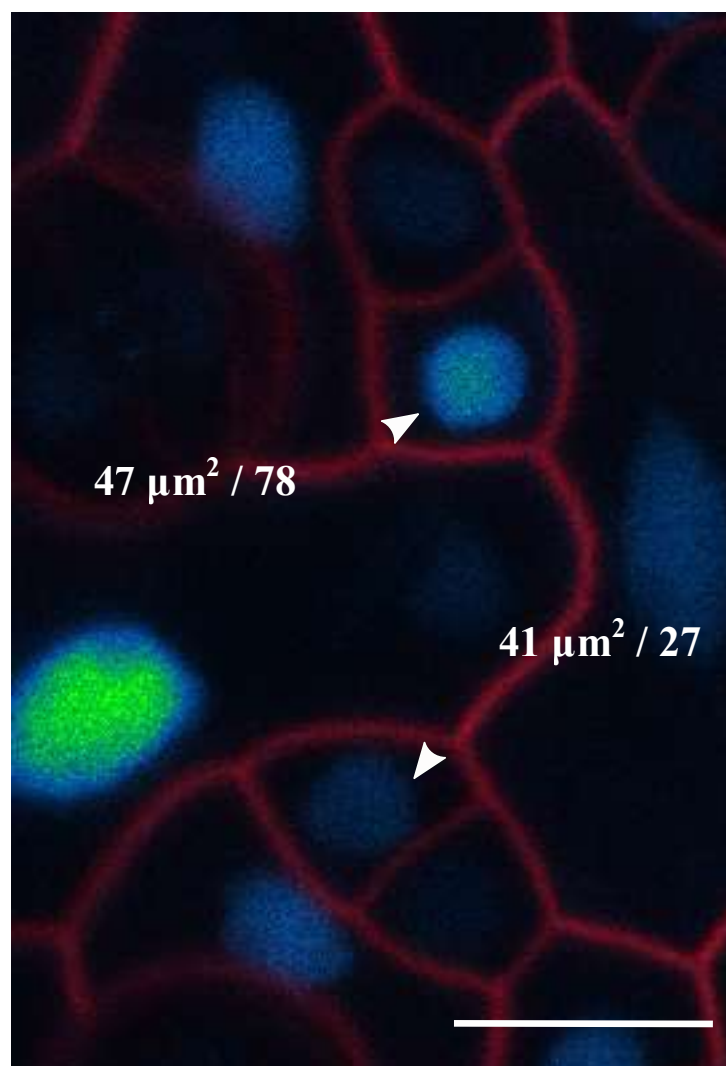
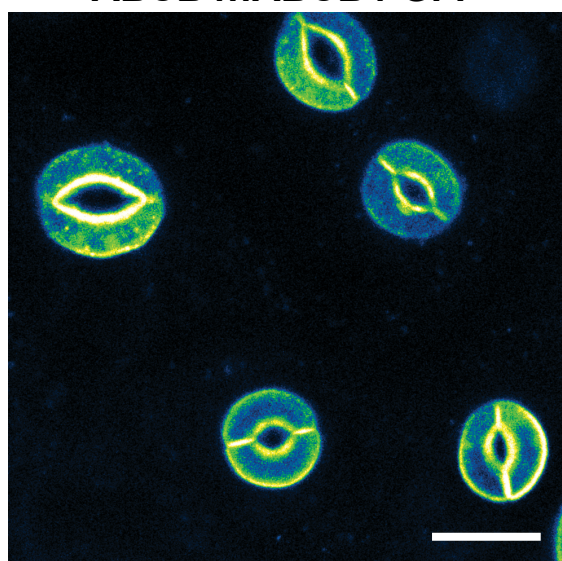
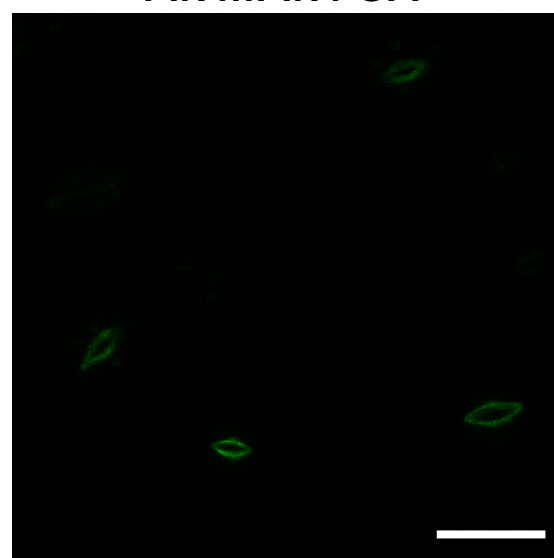
A**DR5::Venus-NLS****B****C****ABCB4::ABCB4-GFP****D****PIN4::PIN4-GFP**

Fig. S3. DR5 signal distribution in the 3rd leaf. (A) Distribution of DR5::Venus-NLS marker within the abaxial side of the 3rd leaf in two-week-old *Arabidopsis*. Scale bar = 500 μ m. (B) Absolute DR5::Venus-NLS signal intensity in the SLGCs does not correlate with their cell area or developmental stage. Arrows indicate examples of two SLGCs in stage 1 with similar cell area but different nuclear DR5 signal intensity. Cell walls are stained with propidium iodide. Scale bar = 10 μ m. (C) Localization of ABCB4::ABCB4-GFP in the epidermal cells of the 3rd leaf in *Arabidopsis*. Scale bar = 10 μ m. (D) Localization of PIN4::PIN4-GFP in the epidermal cells of the 3rd leaf in *Arabidopsis*. Scale bar = 10 μ m.

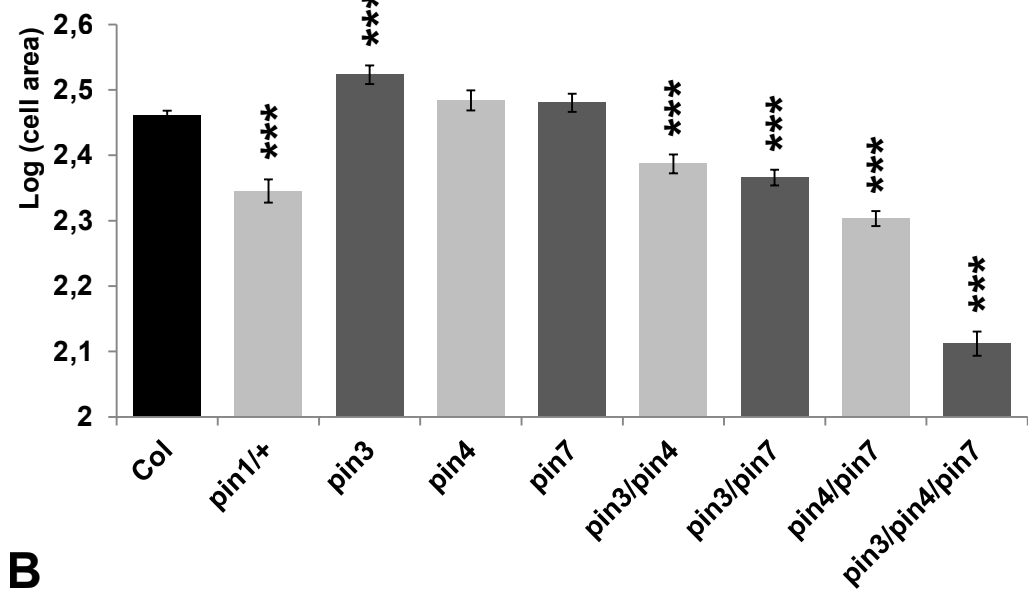
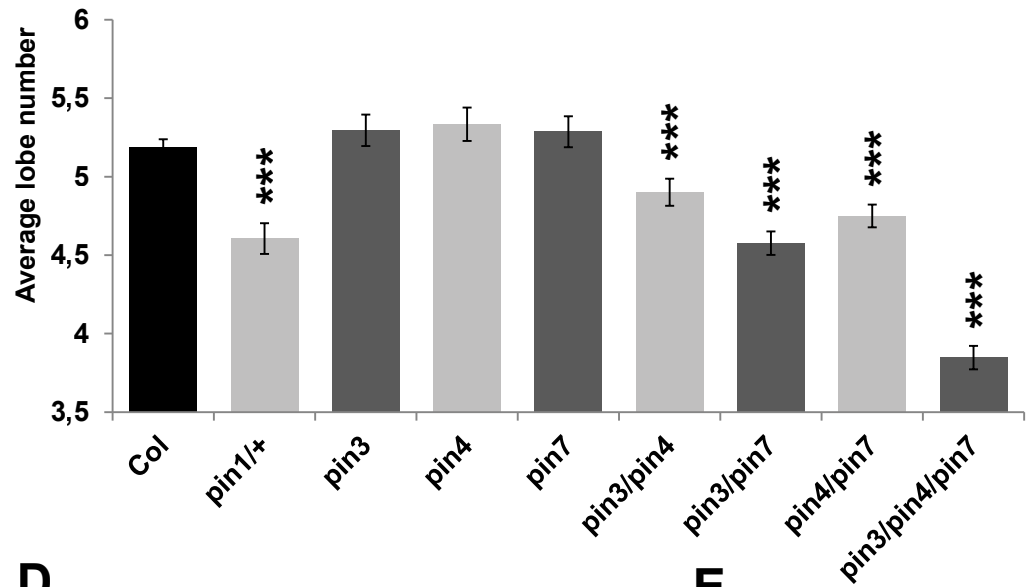
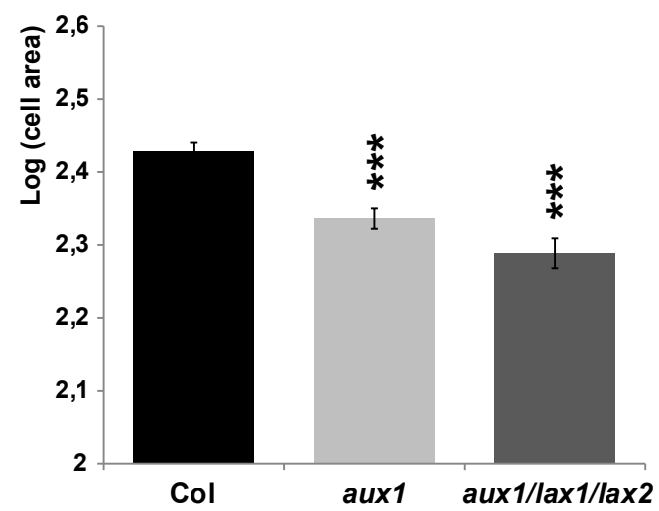
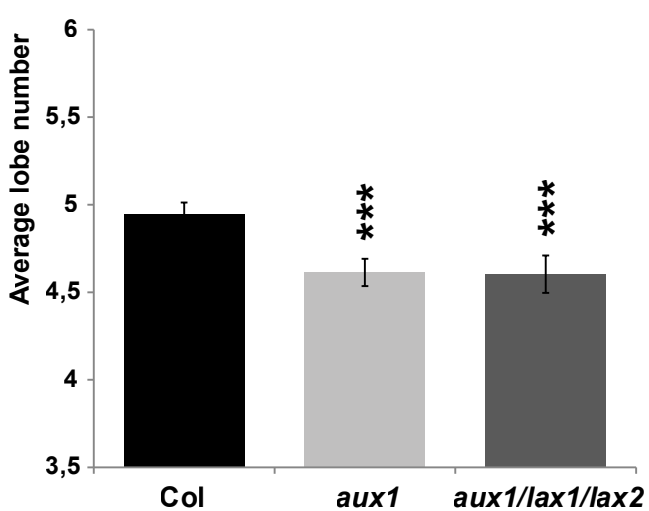
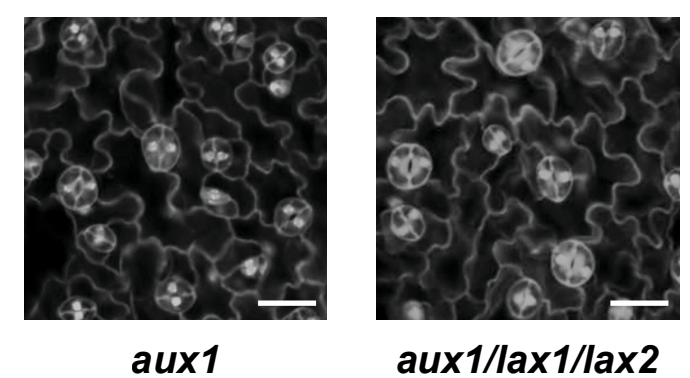
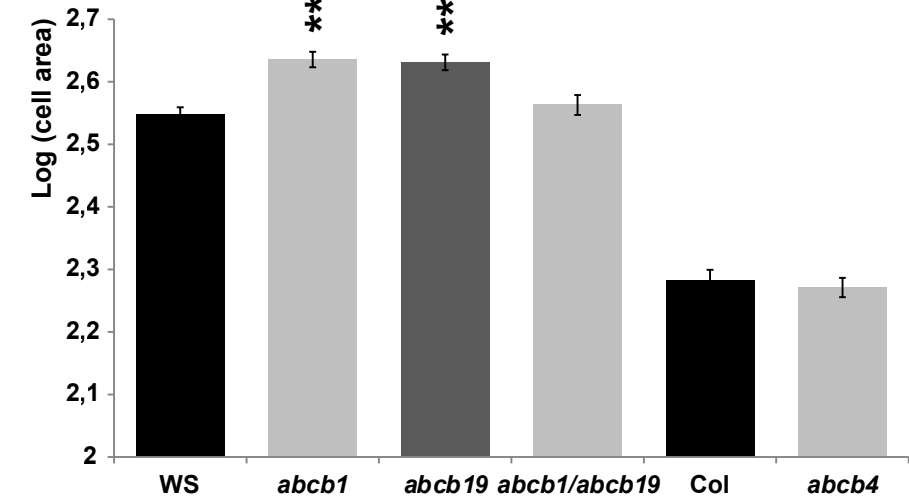
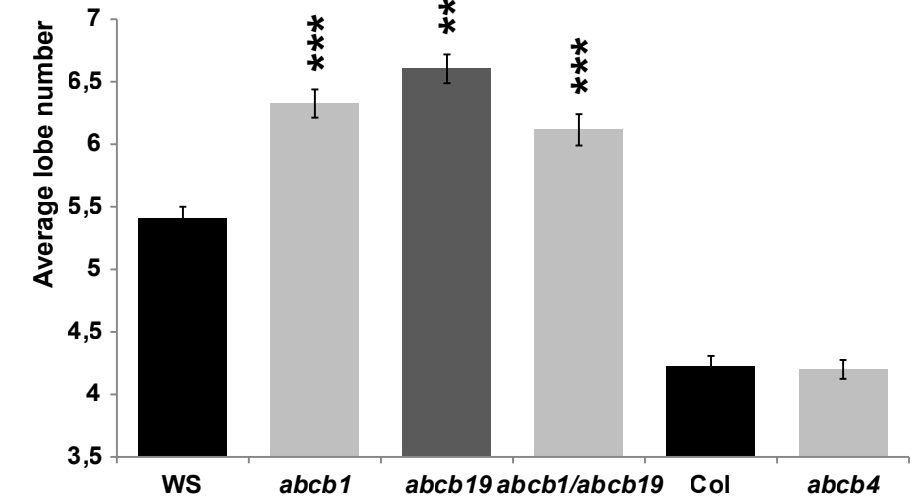
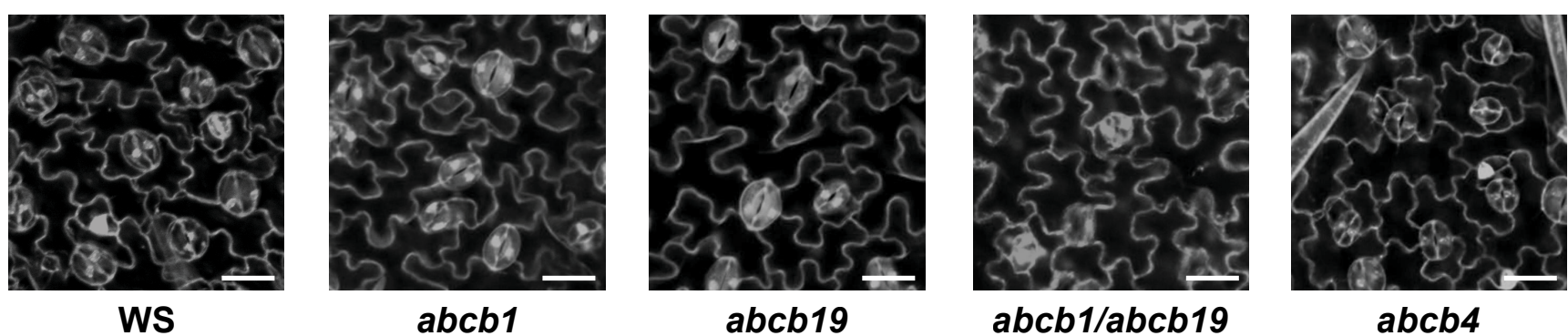
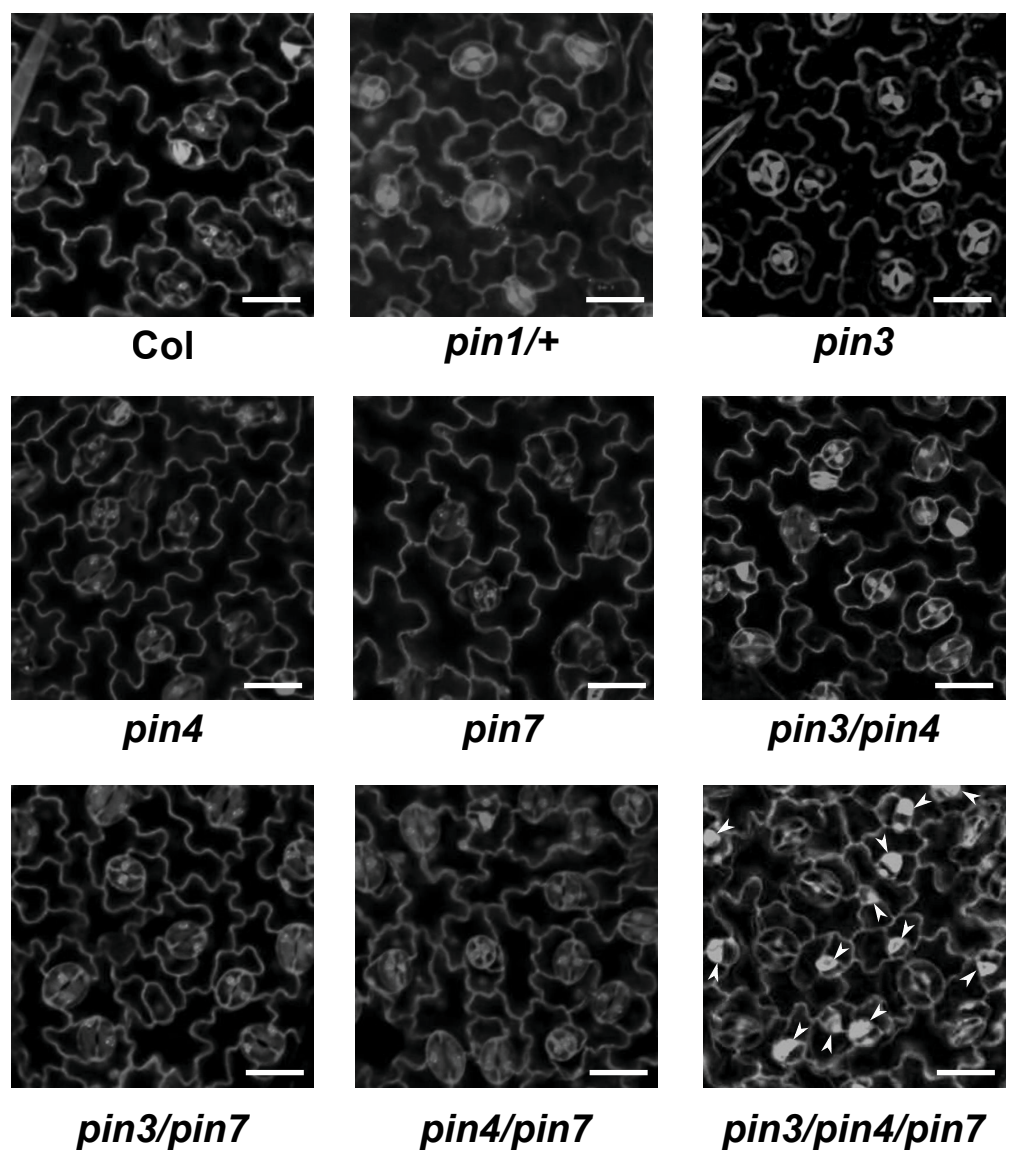
A**B****D****E****F****G****H****I****C**

Fig. S4. Auxin transporter mutants exhibit defects in pavement cell shape. (A) Graph representing the log cell areas of analysed cells of the 3rd leaf in two-week-old *Arabidopsis* in wild type (Col) and *pin* mutants. (B) Graph representing the average lobe number of analysed cells in wild type (Col) and *pin* mutants. (A-B) n = 970 (Col), 679 (*pin1/+*), 791 (*pin3*), 757 (*pin4*), 806 (*pin7*), 822 (*pin3/pin4*), 1028 (*pin3/pin7*), 1193 (*pin4/pin7*) and 644 (*pin3/pin4/pin7*) cells. (C) Representative images of pavement cells in different auxin exporter mutants. Arrowheads showing the increased number of meristemoid cells in *pin3/pin4/pin7/* mutant. (D) Graph representing the log cell areas of analysed cells of the 3rd leaf in two-week-old *Arabidopsis* in wild type (Col) and *aux1* and *aux1/lax1/lax2* mutants. (E) Graph representing the average lobe number of analysed cells in wild type (Col) and *aux1* and *aux1/lax1/lax2* mutants. (D-E) n = 1331 (Col), 925 (*aux1*) and 483 (*aux1/lax1/lax2*) cells. (F) Representative images of pavement cells in auxin importer mutants. (G) Graph representing the log cell areas of analysed cells of the 3rd leaf in two-week-old *Arabidopsis* in wild type (Col) and *abcb* mutants. (H) Graph representing the average lobe number of analysed cells in wild type (Col) and *abcb* mutants. (G-H) n = 982 (WS), 887 (*abcb1*), 914 (*abcb19*), 705 (*abcb1/abcb19*), 521 (Col) and 772 (*abcb4*) cells. (I) Representative images of pavement cells in auxin exporter mutants. Error bars correspond to \pm s.e. Statistics were performed to compare mutants to wild type using Wilcoxon test (***P < 0.001). Scale bar = 20 μ m.

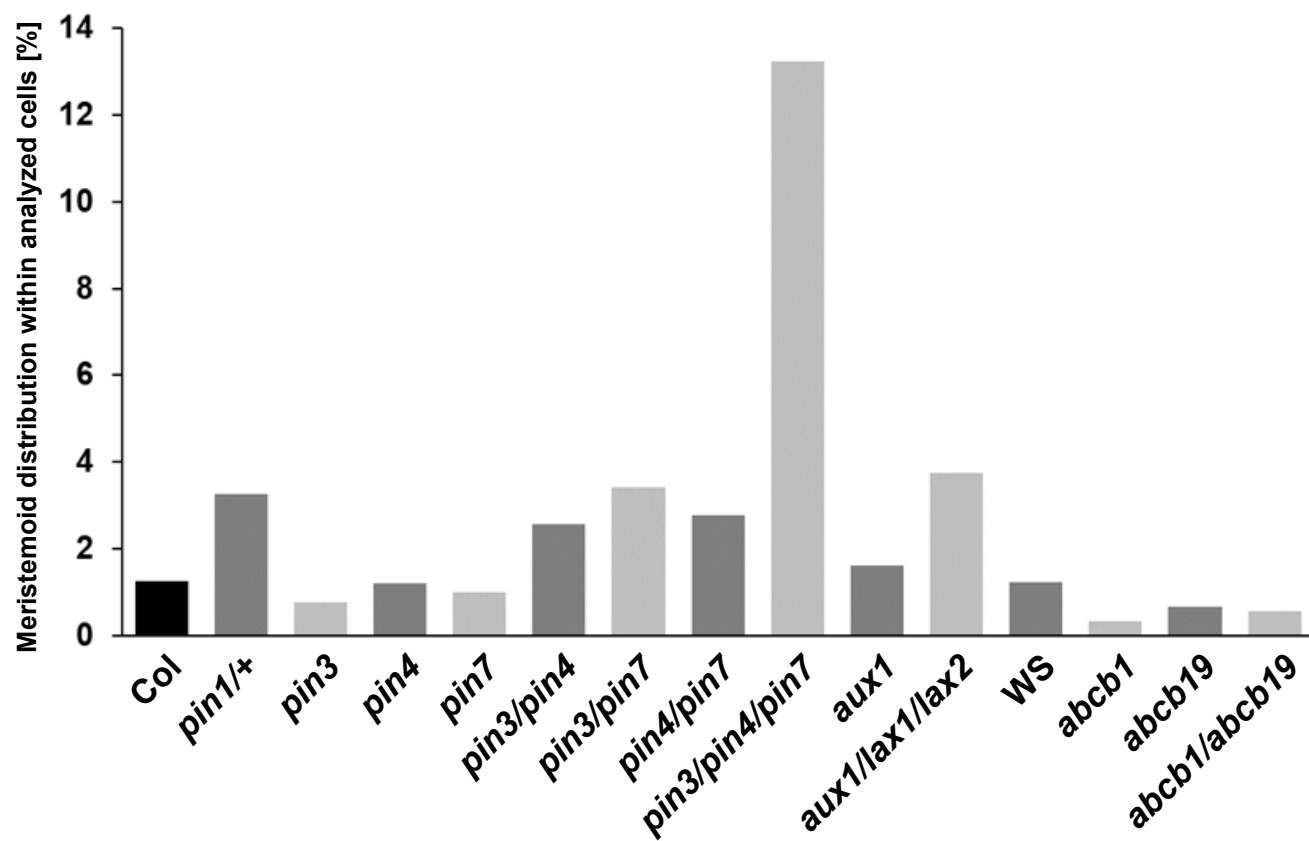
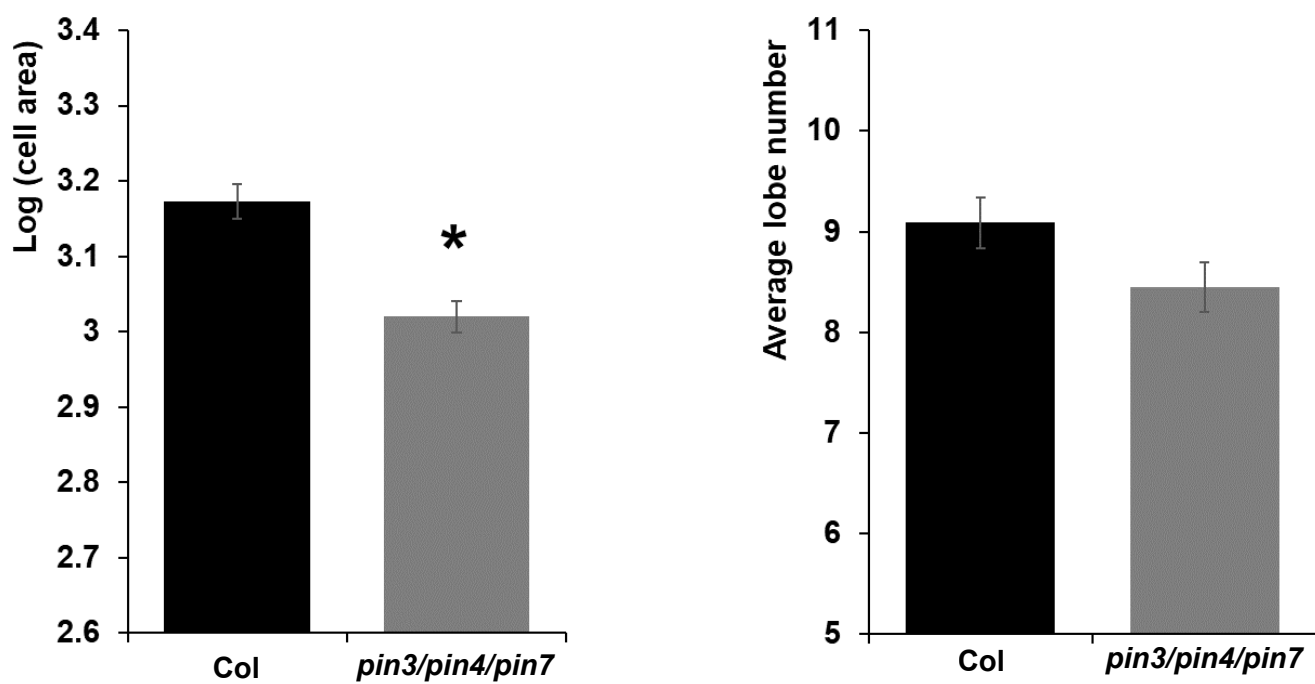
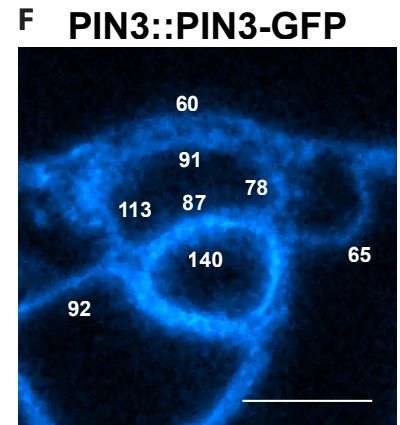
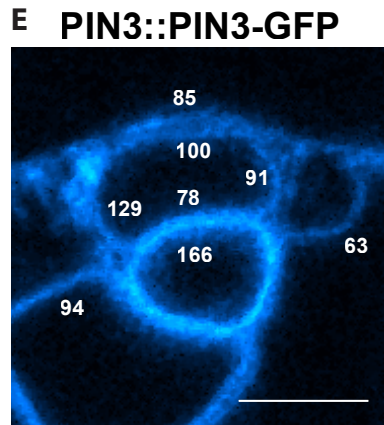
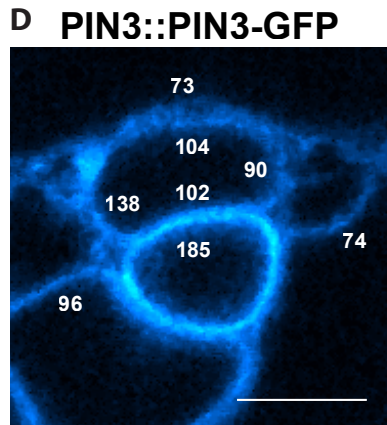
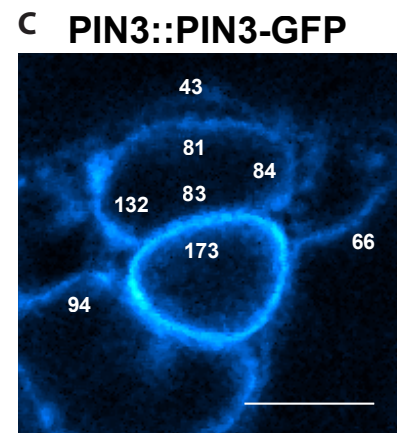
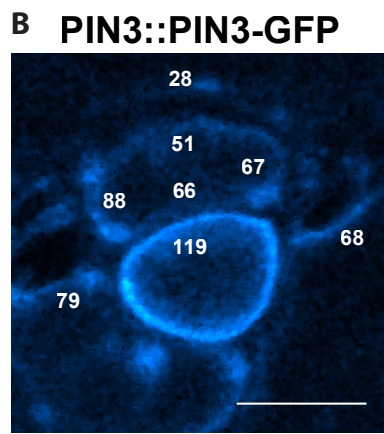
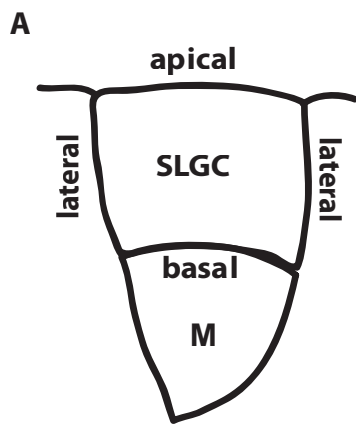
A**B**

Fig. S5. *pin3/4/7* triple mutant shows no difference in lobe number compared to wild type in cotyledon pavement cells. (A) Quantification of distribution of meristemoids within the population of cells analyzed for Fig. S4. (B) Graphs showing log cell area and average lobe number of analysed cells of the cotyledons of 10-day-old *Arabidopsis* in Columbia wild type (Col) and *pin3/4/7* mutants. n = 430 (Col) and 549 (*pin3/4/7*). Error bars correspond to \pm s.e. Statistical significance compared to wild type tested by Wilcoxon test (*P < 0.05)



G

	SLGC-Basal	Meristemoid	SLGC-Apical	Neighbour	SLGC-Lateral-L	Neighbour	SLGC-Lateral-R	Neighbour
Signal intensity B)	66.053	119.930	51.136	28.374	88.617	79.474	67.121	68.997
Signal intensity C)	83.545	173.606	81.708	43.599	132.623	94.979	84.328	66.384
Signal intensity D)	102.445	185.392	104.216	73.938	138.726	96.808	90.212	74.012
Signal intensity E)	78.485	166.272	100.190	85.785	129.264	94.968	91.597	63.566
Signal intensity F)	87.329	140.700	91.953	60.879	113.767	92.416	78.509	65.064
Average	83.571	157.180	85.841	58.515	120.599	91.729	82.353	67.605

Fig. S6. Example of quantification of PIN3-GFP signal intensity measurements at the membranes of SLGC and meristemoid after plasmolysis. (A) Scheme representing stage 1 SLGC with apical, basal and lateral membranes indicated. M – meristemoid. (B-F) Single plane images (slices) of a Z-scan of PIN3::PIN3-GFP (slice thickness = 1 μm). Numbers represent signal intensity at that particular membrane. (G) Quantification of GFP signal distribution of PIN3::PIN3-GFP at the indicated membranes of SLGC and neighbouring cells for each image in (B-F). L – left; R – right. Scale bar = 10 μm .

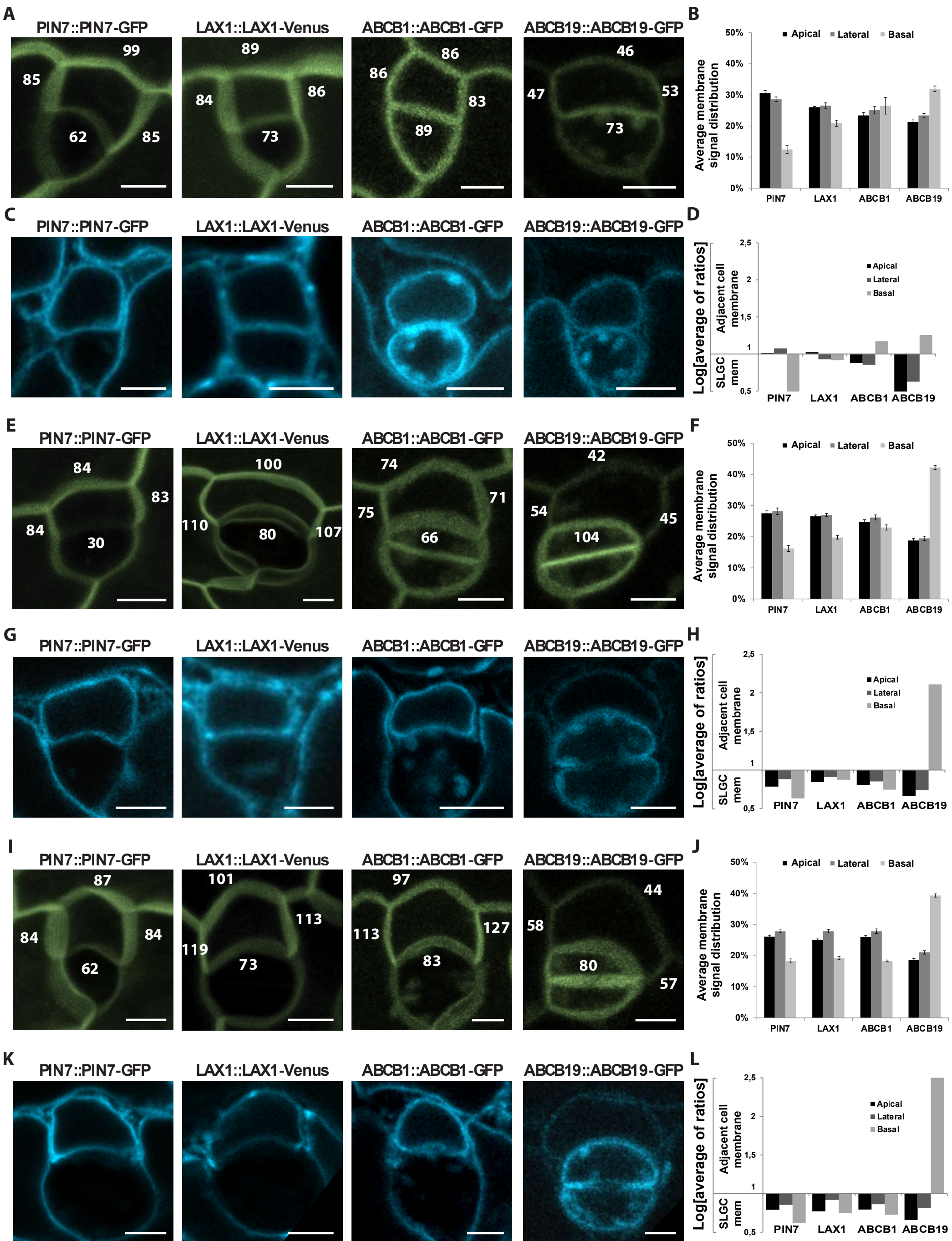
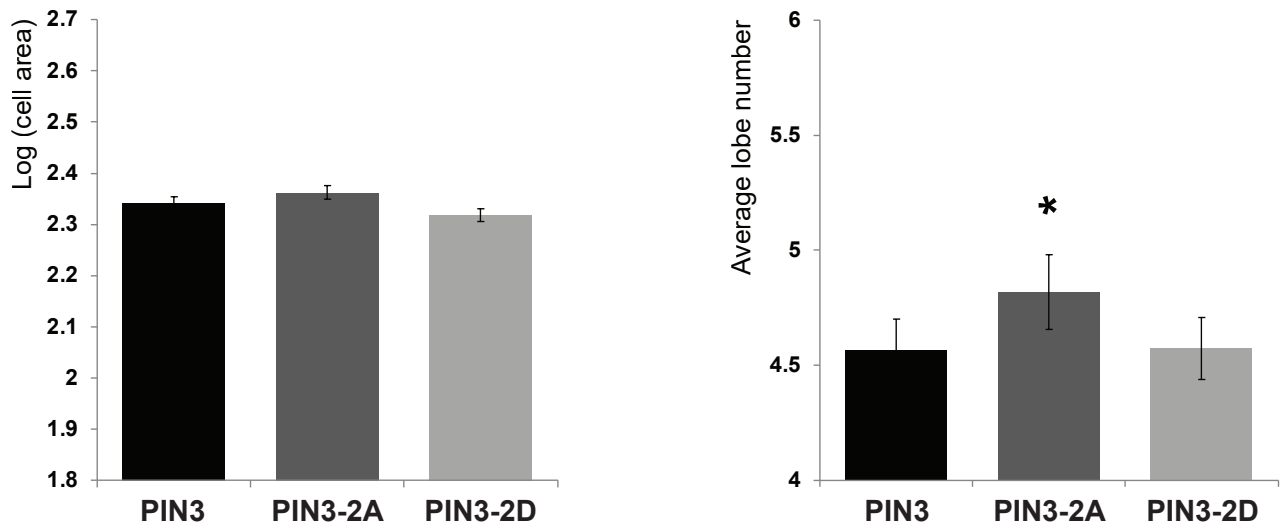
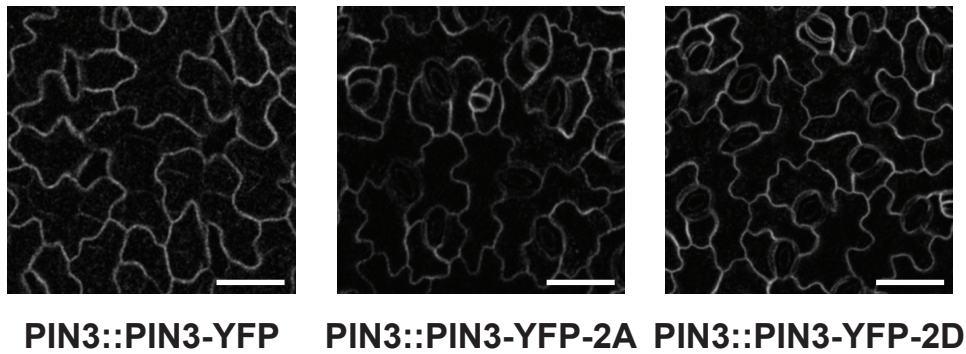


Fig. S7. Localization and distribution of auxin transporters on SLGC and adjacent cell membranes. (A) Maximal intensity projections of Z-scans of different auxin transporter markers in SLGCs from stage 1. Numbers represent quantified Venus/GFP signal intensity at the membranes. (B) Quantification of Venus/GFP signal distribution of different auxin transporter markers at the membranes of SLGCs from stage 1. (C) Representative single plane images of different auxin transporter markers in SLGCs at stage 1 after plasmolysis. (D) Quantification of Venus/GFP signal distribution of different auxin transporter markers at the membranes of SLGCs from stage 1 and adjacent cells after plasmolysis. (E) Maximal intensity projections of Z-scans of different auxin transporter markers in SLGCs from stage 2. Numbers represent quantified Venus/GFP signal intensity at the membranes. (F) Quantification of Venus/GFP signal distribution of different auxin transporter markers at the membranes of SLGCs from stage 2. (G) Representative single plane images of different auxin transporter markers in SLGCs from stage 2 after plasmolysis. (H) Quantification of Venus/GFP signal distribution of different auxin transporter markers at the membranes of SLGCs from stage 2 and adjacent cells after plasmolysis. (I) Maximal intensity projections of Z-scans of different auxin transporter markers in SLGCs from stage 3. Numbers represent quantified Venus/GFP signal intensity at the membranes. (J) Quantification of Venus/GFP signal distribution of different auxin transporter markers at the membranes of SLGCs from stage 3. (K) Representative single plane images of different auxin transporter markers in SLGCs from stage 3 after plasmolysis. (L) Quantification of Venus/GFP signal distribution of different auxin transporter markers at the membranes of SLGCs from stage 3 and adjacent cells after plasmolysis. Values of two lateral membranes from one SLGC were averaged. Values from plasmolysis were log transformed to reduce skewness, log = 1 represents equal distribution of the signal between membranes of SLGC and adjacent cell. Apical, lateral and basal refer to SLGC membranes shown in Fig.s 4A, 4H and 4O. Scale bar = 10 μ m.

A**B**

PIN3::PIN3-YFP

PIN3::PIN3-YFP-2A

PIN3::PIN3-YFP-2D

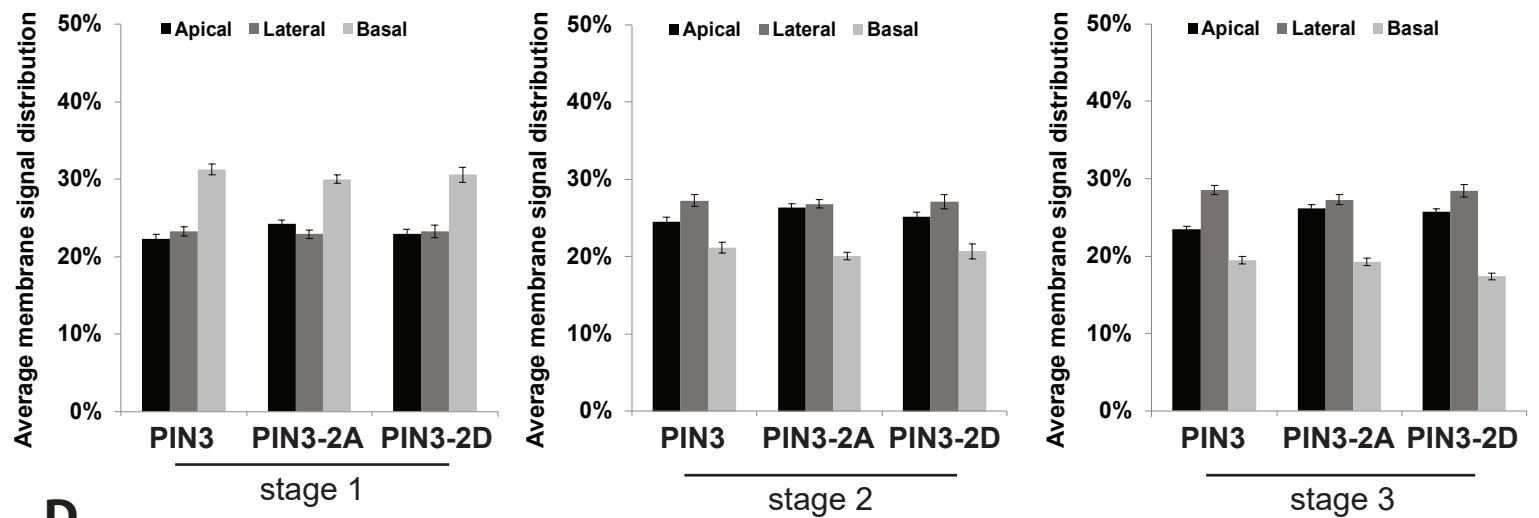
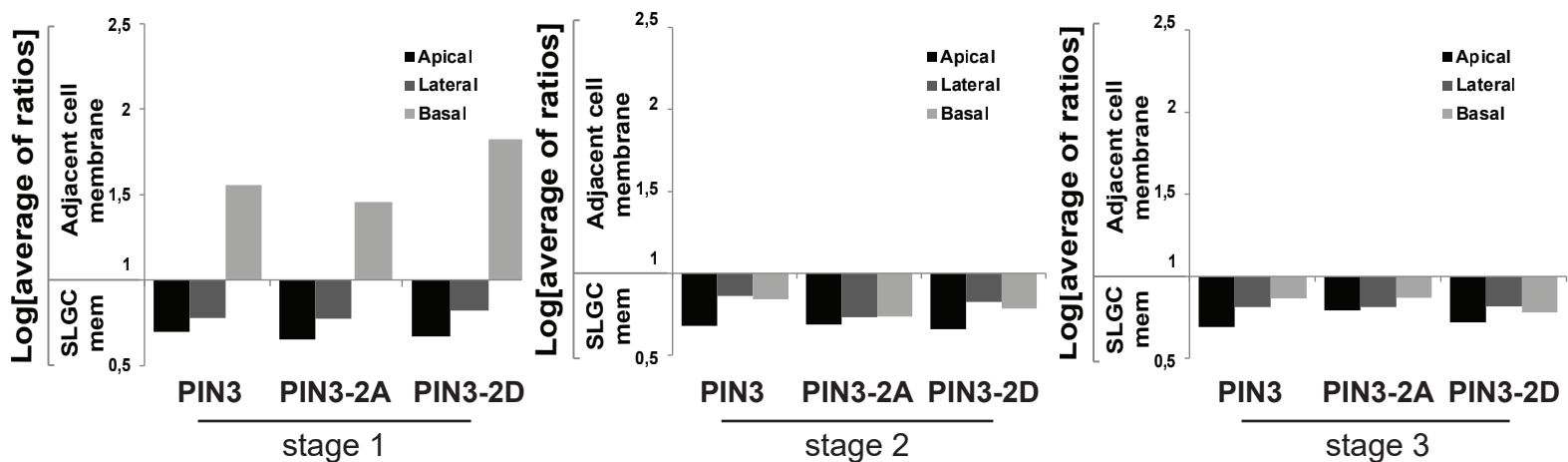
C**D**

Fig. S8. PIN3 phosphorylation mutants display only minor defects in pavement cell shape. (A) Graphs representing the log cell area and average lobe number of analyzed cells of the 3rd leaf in two-week-old *Arabidopsis* in wild type PIN3::PIN3-YFP (PIN3) and PIN3 phosphorylation mutants 2A (non-phosphorylated variant) and 2D (constitutively phosphorylated variant). n = 546 (PIN3-YFP), 480 (PIN3-YFP-2A), and 698 (PIN3-YFP-2D). (B) Representative images of pavement cells in wild type and different PIN3 phosphorylation mutants. (C) Quantification of PIN3-YFP signal distribution at the membranes of SLGCs from stage 1, stage 2 and stage 3 in the PIN3 phosphorylation mutants. (D) Quantification of PIN3-YFP signal distribution at the membranes of SLGCs from stage 1, stage 2 and stage 3 and adjacent cells after plasmolysis in the PIN3 phosphorylation mutants. Values of two lateral membranes from one SLGC were averaged. Values from plasmolysis were log transformed to reduce skewness, log = 1 represents equal distribution of the signal between membranes of SLGC and adjacent cell. Apical, lateral and basal refer to SLGC membranes shown in Fig.s 4A, 4H and 4O. Error bars correspond to \pm s.e. Statistical significance compared to DMSO mock-treated cells or PIN3 tested by Wilcoxon test (*P < 0.05). Scale bar = 20 μ m.

PIN1 (pin1-5-Fw)	AACTGGCTTCACAGCAGAAAG
PIN1 (pin1-5-Rv)	TCAACAAAAAGGGCATTGTTC
PIN3 (pin3-5 Fw)	CCCATCCCCAAAAGTAGAGTG
PIN3 (pin3-5 Rv)	ATGATACACTGGAGGACGACG
PIN4 (pin4-3 Fw)	AACCGGTACGGGTGTTTCAACTA
PIN4 (pin4-3 Rv)	GCCATTCCAAGACCAGCATCT
PIN4 (pin4-3 En)	GAGCGTCGGTCCCCACACTTCTATAC
PIN7 (pin7-1 Fw)	AAATCCGATCAAGGCGGTG
PIN7 (pin7-1 Rv)	CGTCGAATTTCCGCAAGC
PIN7 (pin7-1 Ds5)	ACGGTCGGGAAACTAGCTCTA
PIN7 (pin7-2 Fw)	CTCTTTTGCAAACACAAACGG
PIN7 (pin7-2 Rv)	GGTAAAGGAAGTGCCTAACGG
AUX1 (aux1-21 Fw)	CCGTACTCGTTTAGTCAACTAGGAATG
AUX1 (aux1-21 Rv)	GAGGCAATGGCTAAGTACCAAG
LAX1 (lax1 Fw)	ATATGGTTGCAGGTGGCACA
LAX1 (lax1 Rv)	GTAACCGGCAAAAGCTGCA
LAX2 (lax2 Fw)	ATGGAGAACGGTGAGAAAGCAGC
LAX2 (lax2 Rv)	CGCAGAAGGCAGCGTTAGCG
Border lax	AAGCACGACGGCTGTAGAATAG
ABCB1 (abcb1-Fw)	CTATAGAAACGAGAAGCTGGCCTTC
ABCB1 (abcb1-Rv)	GCTGCACCATTGGCTGAGACC
ABCB1 (BAR6)	GATAGAGCGCCACAATAACAAACAA
ABCB19 (abcb19 Fw)	CTTTGATACTGATGCTAGAACTGGTG
ABCB19 (abcb19 Fw)	GATACAAATCCAACACTAATCCCGCC
ABCB19 (JL-202)	CATTTTATAATAACGCTGCGGACATCTAC

Supplementary table 1 – List of primers used for genotyping